Soft Matter

Accepted Manuscript

This article can be cited before page numbers have been issued, to do this please use: G. Nava, F. Carducci, R. Itri, J. S. Yoneda, T. Bellini and P. Mariani, *Soft Matter*, 2019, DOI: 10.1039/C8SM02616E.

ROYAL SOCIETY OF CHEMISTRY

rsc.li/soft-matter-journal

ROYAL SOCIETY OF CHEMISTRY
View Article Online
DOI: 10.1039/C8SM02616E

Soft Matter

COMMUNICATION

Quadruplex Knots as Network Nodes: Nano-Partitioning of Guanosine Derivates in Supramolecular Hydrogels

Received 00th January 20xx,
Accepted 00th January 20xx

DOI: 10.1039/x0xx00000x

www.rsc.org/

Giovanni Nava[a], Federica Carducci[b], Rosangela Itri[c], Juliana Sakamoto Yoneda[c], Tommaso Bellini*[,a] and Paolo Mariani*[,b]

Aqueous solutions of guanosine-5'-monophosphates (GMP) – known to form G-quadruplexes and liquid crystal phases – can be induced to turn into high water content gels by the addition of guanosine (Gua). By a combination of Light Scattering (LS) and AFM we show that Gua/GMP hydrogels are microscopically heterogeneous, formed by Gua-rich disordered microcoils of intertwined filaments ("knots") connected by GMP-rich long linear threads. The different thermal stability of knots and threads controls the gel transition.

Introduction

High water content gels resulting from the self-assembly of small biomolecules have been a topic of constant interest in the last decades because of their novel structural motifs and because of their potential for biotechnological applications[1–3]. Among them, the recently emerging hydrogels made of fibril-forming ultrashort peptides[3–6] appear attractive systems because of their simple constituents and their intrinsic biocompatibility. Hydrogels based on small biomolecules have recently emerged also in the context of nucleic acids. While DNA gels have been studied for long time[7–10], it was only recently shown that hydrogels can also be obtained in solutions of guanosine derivatives (G)[11–13]. Specifically, it was found that mixtures of guanosine (Gua) and guanosine 5'-monophosphate dipotassium salt (GMP, see Fig. 1A) form stable hydrogels at total concentration c_G 10-100 mg/ml (i.e. ca. 1 - 7% v/v) and at Gua/GMP molar ratio (X) in the range 0.2 – 2[11,13]. The gelation concentration and thermal stability were observed to depend on X, as exemplified in Fig. 1D for the case of c_G = 50 mg/ml[13]. Because of their simple biomolecular

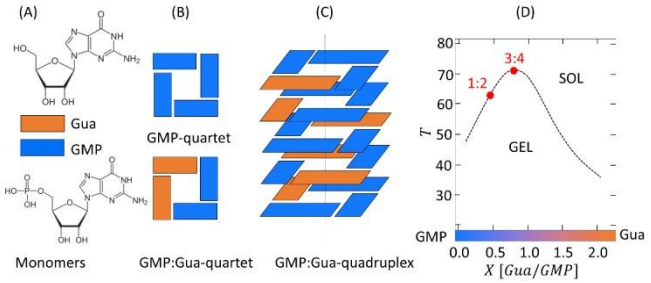

Fig 1: (A) guanosine (Gua) and guanosine 5'-monophosphate (GMP) self-assemble into G-quartets (B), which in turn stack into G-quadruplexes (C). D: temperature-composition (T-X) phase diagram of Gua/GMP mixtures[5].

[a] Dipartimento di Biotecnologie Mediche e Medicina Traslazionale, Università di Milano, via Vanvitelli 32, 20129 Milano, Italy.
[b] Dipartimento di Scienze della Vita e dell'Ambiente, Università Politecnica delle Marche, via Brecce Bianche, 60131 Ancona, Italy.
[c] Departamento Física Aplicada, Instituto de Física, Universidade de São Paulo, Sao Paulo, Brazil.

Electronic Supplementary Information (ESI) available: details about AFM and DLS experimental methods; sample preparation and treatment; AFM image analysis. See DOI: 10.1039/x0xx00000x

View Article Online
DOI: 10.1039/C8SM02616B

constituents and tunability, Gua/GMP hydrogels appear as a new class of convenient and promising bio-soft material whose microscopic mechanisms of aggregation and gelation, currently unknown, are worth understanding.

In Gua/GMP hydrogels, the presence of both components is essential to gelation. When dissolved in water in the presence of alkali metal cations (e.g., Na^+ and K^+), GMPs self-assemble into G-quadruplexes, columnar structures of stacked G-quartets stabilized by stacking forces and by cation coordination of neighbouring carbonyls[14]. Charges provide inter-G-quadruplexes repulsion, so that even at high GMP concentration the system remains fluid and orders into cholesteric or columnar liquid-crystalline phases[15]. The electrically neutral Gua is instead poorly water soluble and it easily agglutinates and precipitates. GMP and Gua solubilities in water are 369 mg/mL and 700 mg/L, respectively. When mixed with GMP, the solubility of Gua markedly increases, an observation consistent with its solubilization through its inclusion in the quadruplexes (Fig. 1B and C)[13].

By combining static and dynamic Light Scattering (LS) and Atomic Force Microscopy (AFM), we studied the gel transition in Gua/GMP solutions and unveiled the mechanism by which the complexification of the GMP and Gua leads to dynamic arrest. Experiments were performed on two solutions with equal c_G = 50 mg/ml and ionic strength (280 mM NaCl), and with X = 0.5 (0.099 M GMP, 0.049 M Gua) and X = 0.75 (0.087 M GMP, 0.065 M Gua), herein referred to as "1:2" and "3:4" samples respectively (sample preparation and experimental details in the SI).

LS Study of the Gel Transition

To characterize the gel transition of Gua/GMP solutions and detect the onset of non-ergodicity we performed static and dynamic LS (details in the SI) as a function of temperature (T) on both still and rotating samples[16].

Fig. 2A compares $\langle I \rangle$, the mean intensity of light scattered at an angle of 90° by the 1:2 sample (blue squares) and by a solution of GMP at the same concentration (red squares). $\langle I \rangle$ of the 1:2 sample was measured while rotating the sample, to ensure a proper ensemble averaging as discussed below. The difference is remarkable: at all T, the Gua/GMP mixture scatters at least 10 times more than the GMP solutions, the latter often being close to the background noise. Therefore, all the features of Gua/GMP mixtures that we measured by LS are a consequence of Gua/GMP complexification.

Fig. 2B shows the intensity correlation function $g_2(\tau) = \langle I(t)I(t+\tau)\rangle / \langle I(t)\rangle^2$ of the light intensity scattered at 90° by the 1:2 sample at 75 °C ≤ T ≤ 90 °C. τ is the delay time. In this T interval, the averaging has been performed over time t. $g_2(\tau)$ exhibit the typical features of freely diffusing particles, indicating the presence of suspended molecular clusters, and are well approximated by stretched exponentials:

$$f(\tau) = Aexp\left[-\left(\tau/\tau_0\right)^{\alpha}\right]$$

as shown in Fig. 2C (dashed lines). We find $\alpha \approx 0.85$, indicating that these clusters are slightly polydisperse. The mean hydrodynamic ratio obtained fitting the curves in Fig. 2B is $R_H \approx 400\,nm$, although we find R_H to depend on the thermal history of the sample, indicating that the solubilization of Gua by GMP is, at least partially, resulting from metastable, kinetic dependent assembling. Samples mixed at high T, rapidly cooled at room T, and then brought back to high T have on average smaller radii than those that were slowly cycled (see in Fig. 2C). Radii measured at $T > 75°C$ are in the range of 0.4 – 1.1 μm for the 1:2 sample, and 1.0 – 1.5 μm for the 3:4 sample.

At high T, time averages ensure the exploration of all the configurations of the system. As T is lowered, the correlation functions become instead less well determined. Fig. 2D compares $g_2(\tau)$ at $T = 75\,°C$ with $\langle g_2(\tau)\rangle_E$ measured at $T = 55\,°C$ (red and blue lines, respectively), the latter obtained by averaging independent measurements of $g_2(\tau)$ performed by illuminating different portions of the sample. This procedure of "ensemble averaging", frequently adopted to investigate kinetically arrested systems, such as colloidal, polymeric and chemical gels[17], was necessary because at T ≤ 65 °C the correlation functions are still decaying at $\tau = 1\,s$ and thus simple time averaging does not provide thermodynamic averaging.

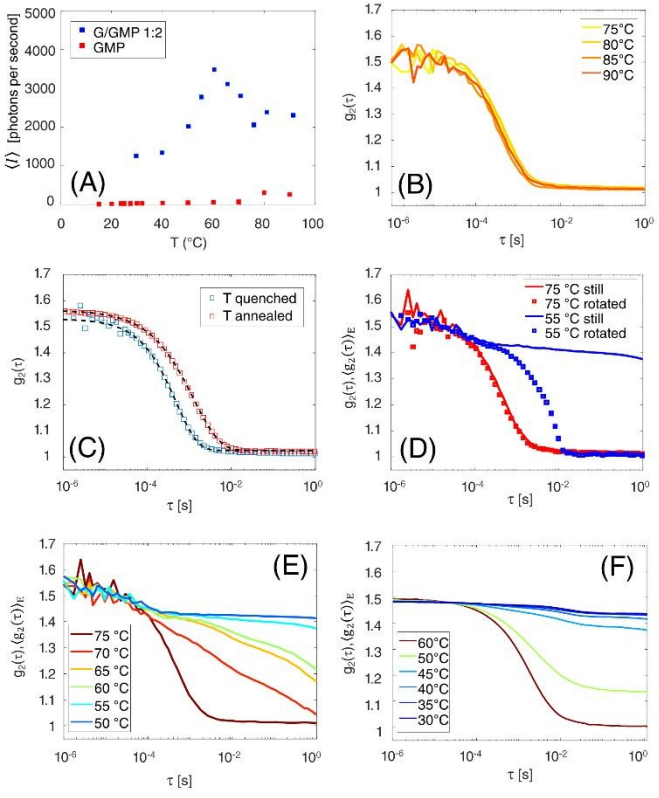

Fig 2: Light Scattering results. (A) Average intensity $\langle I \rangle$ as a function of T for solutions of GMP (red squares) and 1:2 Gua/GMP mixtures (blue squares). (B) Intensity autocorrelations $g_2(\tau)$ at high T for the 1:2 Gua/GMP. (C) $g_2(\tau)$ dependence on thermal history (quenched – blue squares; slow anneal – red squares) fitted with stretched exponentials (dashed lines). (D) $g_2(\tau)$ at T = 55°C (blue line) and high T = 75°C (red line). Both curves were normalized using $\langle I \rangle$ as measured in rotating samples (blue/red squares). (E, F) $g_2(\tau)$ as a function of T for 1:2 (E) and 3:4 (F) Gua/GMP mixtures.

View Article Online
DOI: 10.1039/C8SM02616F

$\langle g_2(\tau)\rangle_E$ in Fig. 2D demonstrates the presence of concentration fluctuations that do not relax in the time of experiments. A simple and effective procedure to appreciate such kinetic arrest by LS, is to measure the correlation function while continuously rotating the sample around its axis, thus effectively mimicking the transformation between conformations and forcing the decorrelation of I(t). In Fig. 2D we show the resulting $g_2(\tau)_R$ for T = 75 °C and T = 55 °C (blue and red dots). At T = 55 °C, this procedure of forced decorrelation leads to a decay amplitude of $g_2(\tau)_R$ much larger than $\langle g_2(\tau)\rangle_E$, an unambiguous demonstration that the small decay of the latter is due to a kinetic arrest at length scale of the optical wavelength. Overall, the 1:2 and the 3:4 samples show analogous behaviour but shifted in T (Figs. 2E and 2F). In both systems, gelation occurs upon cooling through a progressive reduction of the mobility of the molecular clusters that were freely diffusing at high T.

heterogeneity, with lumps and filaments. Filaments, extending up to several μm, show different thicknesses. Line scan analysis (see SI) indicates that the size of thin filaments (2–3 nm) is the typical size of a single G-quadruplex cross-section (2.4 nm[15]), while the size of the thicker ones is compatible with the bundling of more than one quadruplex. Filaments converge into the lumps, which, at a closer inspection, appear as "knots", tangled structures in which the filaments are folded in disordered loop patterns. Noticeable, both 1:2 (Fig. 3B and C) and 3:4 (Fig. 3D) samples present knots of similar size (500-700 nm, see SI) and similar number of lacing wires.

Discussion

The structure emerging from AFM imaging combines with the LS results to clarify the gelation process of Gua/GMP solutions. AFM shows that filaments are compatible with the typical size

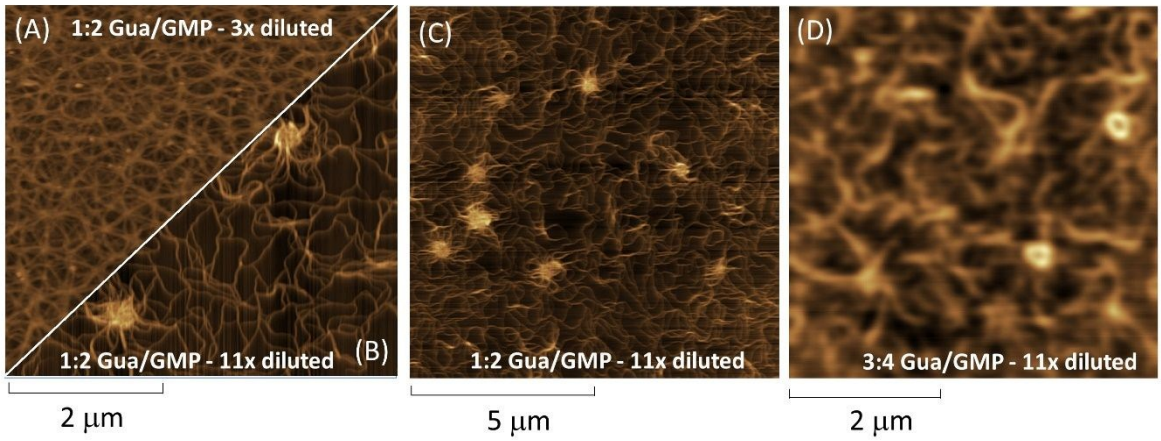

Fig 3: AFM images of: 1:2 hydrogel with 3x dilution (A) and 11x dilution (B); 1:2 sample with 11x dilution, reduced scale (C); 3:4 sample with 3x dilution (D)

AFM Study of the Hydrogel Entanglement at High Dilution

To explore the nature of such thermally stable aggregates, we extended the analysis by AFM that was previously performed on these same hydrogels[13]. AFM observations entail spreading a thin amount of hydrogel on freshly cleaved mica substrates and drying it at room temperature. Since this procedure cannot be easily extended at high T because hydrogels dry too fast and irregularly, we explored instead the regime of high dilution, taking advantage of the fact that G-quadruplexes dissolve either by increasing T or by dilution[13]. AFM observations were performed in dynamic mode and using silicon probes with a resonance frequency ranging from 324 to 369 kHz and scan rates of 0.2–0.5 Hz (more details in the SI) on 1:2 and 3:4 samples which were diluted enough to melt the gel. Fig 3, A to C, shows AFM images from 1:2 hydrogel, prepared at c_G = 50 mg/ml and further diluted 3-fold (c_G = 12.5 mg/ml, Fig. 3A) and 11-fold (c_G = 4.2 mg/ml, Fig. 3B and C). At the lower dilution (Fig. 3A), a high degree of 3D organization on the sub-μm scale is observed while in the highly diluted samples (Fig. 3B and C) the sample topography indicates

of G-quadruplex made of GMP, indicating that this basic self-assembly motif of GMP is preserved even in Gua/GMP mixtures. Gua/GMP filaments are however more flexible and adhesive than those in pure GMP solutions, an effect that must be due to reduction of charge density and the increase of hydrophobicity of G-quadruplexes due to the incorporation of Gua. Flexibility and adhesiveness, already noticeable in filaments in Fig. 3B through side-by-side contacts and bundle formation, become extreme within the knots, suggesting that in these structures the concentration of Gua is larger than in filaments. This notion is supported by the thermal behavior observed by LS. Upon raising T from room temperature, the hydrogel – whose structure might resemble the highly connected 3D network suggested by Fig. 3A, becomes progressively looser – as the depicted in Fig. 3B, eventually transforming into a solution of freely diffusing, thermally stable clusters. We understand this transformation, which takes place at temperatures compatible with the melting of

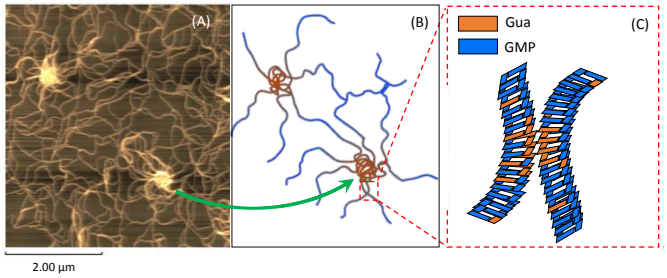

Fig 4: Pictorial description of the nano-segregation taking place in Gua/GMP hydrogels (A) showing their partitioning with color code (B) and the adhesiveness of Gua-doped G-quadruplexes (C).

GMP-quadruplexes[13,15], as the dissolution of the filaments. As GMP solubilizes, the G-quadruplex become enriched by the less soluble Gua, which makes them bend and fold into knots. The hydrodynamic radius measured by LS at high T is consistent with the size of the knots observed by AFM, supporting the notion these are due to the accumulation of Gua, whose much lower solubility makes GMP-stabilized Gua-rich structures thermally stable.

Our understanding, pictorially sketched in Fig. 4, is thus based on the interplay of two basic elements: (i) Gua/GMP *knots*, rich in Gua, which makes them thermally stable; (ii) Gua/GMP *filaments*, rich in GMP, which melt at the T expected for GMP quadruplexes, acting as connectors between the knots.

This picture agrees with the observation that the T dependence of $\langle I \rangle$ is not monotonic (Fig. 2A), which indicates that at 60-70 °C the system has the largest degree of inhomogeneities on the μm length scale. Indeed, upon cooling from T = 75°C, we expect the knots to gain molecular mass through the condensation of GMP into G-quadruplexes-based filaments growing around them, thus inducing a growth in $\langle I \rangle$. As T is further lowered, G-quadruplexes nucleates everywhere in the solution, providing a more extensive solubilizing milieu for Gua, and thus a more homogeneous molecular distribution, a condition which lowers the cross section for the scattering of light.

Conclusions

This work is devoted to the understanding of the molecular mechanism causing the gelation of dilute solutions of Gua and GMP. Our results indicate that these mixtures undergo a nano-partitioning in which GMP-rich regions behave similarly to conventional GMP solutions, forming long columns of G-quartets, while Gua-rich regions are shaped as tangled coils of G-quadruplexes. This partitioning is at the core of the structure of the hydrogel. Thermally stable Gua-rich knots are the nodes of the network, which become connected through thermally reversible GMP-rich filaments. It is worth noticing that this nodes/connector gelation mechanism, relying on the multicomponent nature of the Gua/GMP hydrogels, intrinsically differs from the hydrogels based on short peptides, which are instead typically formed by single biomolecular components. Indeed, although the gelation mechanism of fibril forming short peptide hydrogels has not been clarified in detail yet, it is assumed to be due to a delocalized attraction between the fibrils.

The large coordination number of the nodes, and the reversible structure of the converging filaments, make GMP/Gua hydrogel a new example of a biomolecular transient network[9,18,19].

Conflicts of interest

There are no conflicts to declare.

Corresponding Authors

*E-mail: p.mariani@univpm.it; tommaso.bellini@unimi.it

View Article Online
DOI: 10.1039/C8SM02616E

Funding Sources

R.I. and J.S.Y. are recipients of CNPq (National Council for Scientific and Technological Development, Brazil) research and post-doctoral fellowships. P.M. was CNPq invited researcher (project number 401252/2014-0). T.B. is supported by the "NeOn" project of Regione Lombardia (POR FESR 2014-2020, ID 239047).

Acknowledgment

The authors thank Pietro Ciancaglini and Ivana A. Borin of the Laboratory of Atomic Force Microscopy of the Chemistry Department – FFCLRP – USP (Brazil) for help during AFM measurements.

References

1 E. F. Banwell, E. S. Abelardo, D. J. Adams, M. A. Birchall, A. Corrigan, A. M. Donald, M. Kirkland, L. C. Serpell, M. F. Butler and D. N. Woolfson, *Nat. Mater.*, 2009, **8**, 596–600.

2 S. Zhang, *Nat. Biotechnol.*, 2003, **21**, 1171–1178.

3 W. Y. Seow and C. A. E. Hauser, *Mater. Today*, 2014, **17**, 381–388.

4 G. Fichman and E. Gazit, *Acta Biomater.*, 2014, **10**, 1671–1682.

5 D. J. Pochan, J. P. Schneider, J. Kretsinger, B. Ozbas, K. Rajagopal and L. Haines, *J. Am. Chem. Soc.*, 2003, **125**, 11802–11803.

6 P. Gagni, A. Romanato, G. Bergamaschi, P. Bettotti, R. Vanna, C. Piotto, C. F. Morasso, M. Chiari, M. Cretich and A. Gori, *Nanoscale Adv.*, , DOI:10.1039/c8na00158h.

7 J. B. Lee, Y. H. Roh, S. H. Um, H. Funabashi, W. Cheng, J. J. Cha, P. Kiatwuthinon, D. A. Muller and D. Luo, *Nat. Nanotechnol.*, 2009, **4**, 430–436.

8 S. H. Um, J. B. Lee, N. Park, S. Y. Kwon, C. C. Umbach and D. Luo, *Nat. Mater.*, 2006, **5**, 797–801.

9 G. Nava, Y. Tie, V. Vitali, P. Minzioni, I. Cristiani, F. Bragheri, R. Osellame, L. Bethge, S. Klussmann, E. M. Paraboschi, R. Asselta and T. Bellini, *Soft Matter*, 2018, **14**, 3288–3295.

10 G. Nava, M. Rossi, S. Biffi, F. Sciortino and T. Bellini, *Phys. Rev. Lett.*, 2017, **119**, 078002.

11 E. Yu, D. Nakamura, K. DeBoyace, A. W. Neisius and L. B. McGown, *J. Phys. Chem. B*, 2008, **112**, 1130–1134.

12 G. M. Peters and J. T. Davis, *Chem. Soc. Rev.*, 2016, **45**, 3188–3206.

13 F. Carducci, J. S. Yoneda, R. Itri and P. Mariani, *Soft Matter*, 2018, **14**, 2938–2948.

14 M. Gellert, M. N. Lipsett and D. R. Davies, *Proc. Natl. Acad. Sci.*, 1962, **48**, 2013–2018.

15 S. Bonazzi, M. Capobianco, M. M. De Morais, A. Garbesi, G. Gottarelli, P. Mariani, M. G. Ponzi Bossi, G. P. Spada and L. Tondelli, *J. Am. Chem. Soc.*, 1991, **113**, 5809–5816.

View Article Online
DOI: 10.1039/C8SM02616E

16 J. Z. Xue, D. J. Pine, S. T. Milner, X. L. Wu and P. M. Chaikin, *Phys. Rev. A*, 1992, **46**, 6550–6563.
17 P. N. Pusey and W. Van Megen, *Phys. A Stat. Mech. its Appl.*, 1989, **157**, 705–741.
18 R. Tharmann, M. M. A. E. Claessens and A. R. Bausch, *Phys. Rev. Lett.*, 2007, **98**, 088103.
19 C. Storm, J. J. Pastore, F. C. MacKintosh, T. C. Lubensky and P. A. Janmey, *Nature*, 2005, **435**, 191–194.

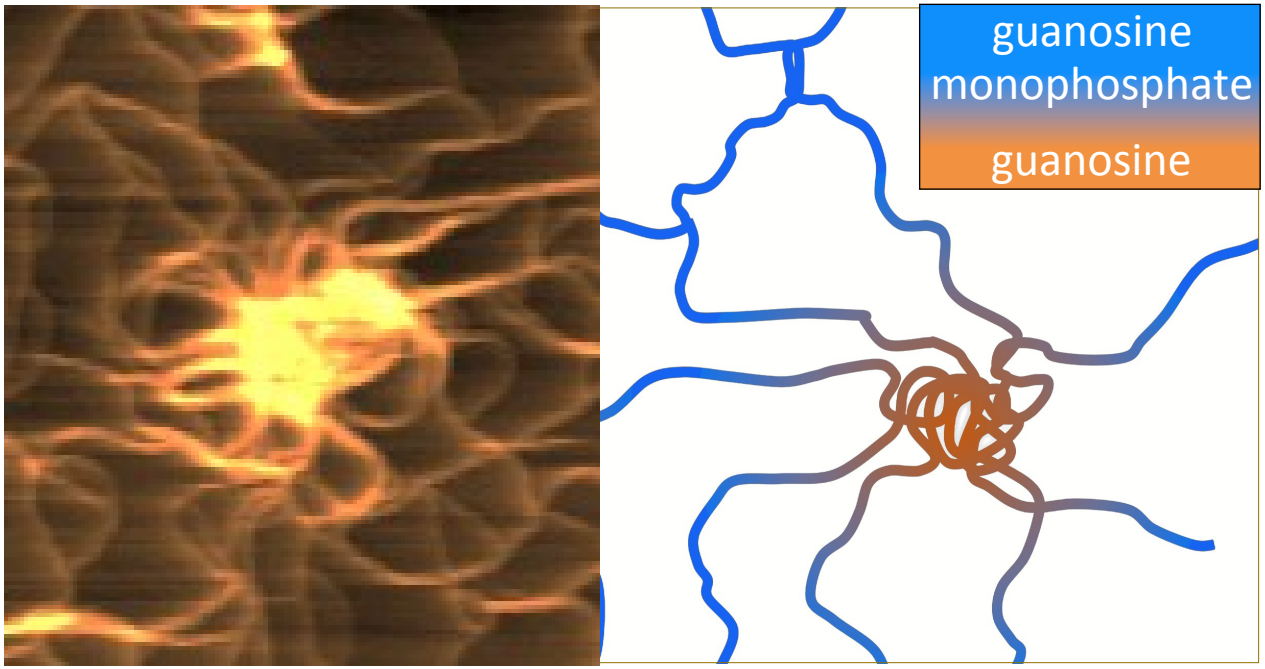

TOC: Gua/GMP hydrogels are formed by disordered microcoils of intertwined filaments (*knots*, rich in gua) connected by long linear GMP-rich *threads*. Gua provides flexibility and thread attraction, responsible for hydrogel stability (AFM image is 2.5 x 2.5 µm).